NMR study of micas, II. Distribution of Fe²⁺, F⁻, and OH⁻ in the octahedral sheet of phlogopites

Jesus Sanz[1]

Groupe de Physico-Chimie Minérale et de Catalyse, University of Louvain
Place Croix du Sud 1, B-1348 Louvain-la-Neuve, Belgium

and William E. E. Stone

Section de Physico-Chimie Minérale (M.R.A.C.-Tervuren)
Place Croix du Sud 1, B-1348 Louvain-la-Neuve, Belgium

Abstract

By studying the NMR signals of protons and fluorine in a series of crystalline phlogopites at various frequencies and angles, it has been possible to differentiate among various octahedral associations. In samples with continuously variable amounts of fluorine and iron, we show that the OH groups, rather than the fluorine ions, are in direct coordination with the iron. This anionic segregation relative to Fe²⁺ is also confirmed by the observation of fluorine pairs, which most probably form homogeneous fluorine domains. This local ordering of octahedral ions is an important parameter in the study of cohesion of layered silicates.

Introduction

Phlogopites belong to the sheet silicate group; their ideal formula is $KMg_3Si_3AlO_{10}(OH)_2$. The Mg^{2+} ions located in the central octahedral sheet of the elementary layer are only slightly substituted by Fe^{2+} ions, whereas the OH groups may be replaced by F^- ions to various degrees. It is well known that the nature of the isomorphous substituents within the octahedral sheet of micas is a determinant factor in the vermiculitization process of these minerals; in particular, when the fluorine content increases, the ease with which K^+ can be replaced by Na^+ decreases. The F^- and H^+ nuclear magnetic resonance spectra of ten phlogopite samples have been examined in order to understand how the nature of the octahedral sheet influences this process.

In the octahedral sheet, two different cation sites are possible, depending on whether the OH groups are in *cis* (*M2* site) or *trans* position (*M1* site) (Fig. 1). These OH groups are located on the π symmetry plane and are coordinated to one *M1* cation in the plane and to two *M2* cations located on both sides of the plane.

We will show that from the H^+ and F^- NMR signals, it is possible to characterize the distribution of the Fe^{2+} ion with respect to the anions OH^-, F^- as a result of the large paramagnetic influence of the Fe^{2+} on the nuclear signals. We will also show that the strong nuclear dipolar interaction between F^- ions belonging to the same octahedra leads to information concerning the degree of order which exists in the octahedral distribution of this ion. These results indicate ionic segregation within the octahedral sheet and therefore suggest the existence of short-range order which supplements the picture of average structures given by X-ray diffraction studies.

Experimental

The samples studied (for chemical composition see Table 1) are part of a collection of micas whose weathering properties had been determined previously in our laboratory (Rousseaux *et al.*, 1973). The samples were chosen such that the fluorine content varied continuously between 0.7 to 5.2 percent (by weight), the paramagnetic impurities, essentially Fe^{2+} ions, being in the range 0.2 to 3 percent. The samples formed by superposing individual platelets (10 × 10 mm) were cut from large natural mica plates, on which the *a* and *b* axis orientations had been determined beforehand. Altered or twinned regions were carefully avoided.

---

[1] Present address: C.S.I.C. Serrano 115 Dpdo, Madrid 6, Spain

Table 1. Sample compositions[1]

	Si^{4+}	Al^{3+}	Al^{3+}	Ti^{4+}	Fe^{3+}	Fe^{2+}	Mg^{2+}	Mn^{2+}	Li^+	Ca^{2+}	Na^+	K^+	O^{2-}	OH^-	F^-
P-2	2.74	1.26	0.18	0.05	0.01	0.16	2.55	–	0.01	0.05	0.06	0.85	9.93	1.92	0.15
P-21	2.74	1.26	0.15	0.06	0.10	0.17	2.41	–	0.39	–	0.11	0.85	10.22	1.48	0.30
P-4	2.90	1.10	0.16	0.08	0.04	0.10	2.68	–	0.01	0.01	0.07	0.88	10.35	1.19	0.46
P-12	2.88	1.12	0.27	0.05	0.02	0.02	2.74	–	0.01	0.01	0.04	0.91	10.42	1.09	0.49
P-8	2.84	1.16	0.11	0.07	–	0.02	2.83	–	–	0.03	0.06	0.87	10.16	1.21	0.63
P-6	2.92	1.08	0.12	0.06	0.01	0.05	2.86	–	–	0.04	0.05	0.90	10.34	0.92	0.74
P-13	2.79	1.21	0.01	0.02	–	0.15	2.64	–	0.01	0.07	0.03	0.93	9.61	1.60	0.79
P-15	2.88	1.12	0.15	0.07	0.01	0.04	2.73	–	0.03	0.02	0.02	0.96	10.24	1.02	0.74
P-16	2.83	1.17	0.05	0.03	0.04	0.07	2.90	–	–	0.01	0.03	0.93	10.14	0.89	0.97
P-18	3.00	1.00	0.06	0.02	0.03	0.17	2.73	0.01	0.03	0.03	0.04	0.95	10.26	0.57	1.16

[1] J.M. Rousseaux et al. (1973).

NMR spectra were obtained at room temperature with a Varian continuous-wave crossed-coiled spectrometer working at different fixed frequencies (14, 54.6, and 60 MHz). In order to obtain signal-to-noise ratios around 30 to 50, the spectra were signal-averaged. The paramagnetic influence on the nuclear spectra increases with frequency. Therefore, experiments run at high frequency allowed us to study the influence of varying Fe^{2+} contents on the H^+ and F^- spectra. These experiments were also useful in identifying the various interactions responsible for the observed spectra. Experiments at low frequency (14 MHz) were run at various angles around the b axis, because of better resolution in this plane, in order to provide information concerning the diamagnetic interactions.

Results

Proton signal—a axis

H^+ gives rise to a large symmetrical Gaussian line accompanied, when the iron content is above one percent, by small side lines, whose intensity increases with the iron concentration.

Figure 2 shows the second moment of the principal line obtained from the peak-to-peak value of the experimental first derivative spectra, at 60 MHz, as a function of iron content. The line-width is essentially dominated by the paramagnetic interaction which gives rise to the expected parabolic shape. By working at lower frequencies, which decreases the paramagnetic contributions to the width of the line, the dipolar diamagnetic part of the interaction remains more or less constant for all samples.

The position of the side-lines with respect to the central line varies as a function of the orientation of the sample with respect to the applied magnetic field. It also varies linearly with the applied field, as is to be expected for averaged electronic moments obeying Curie's law. An analysis of these side-lines has clearly shown (Sanz and Stone, 1977) that they are due to OH^- groups, which are first-nearest neighbors (*i.e.* 2.7A) to the Fe^{2+} ions.
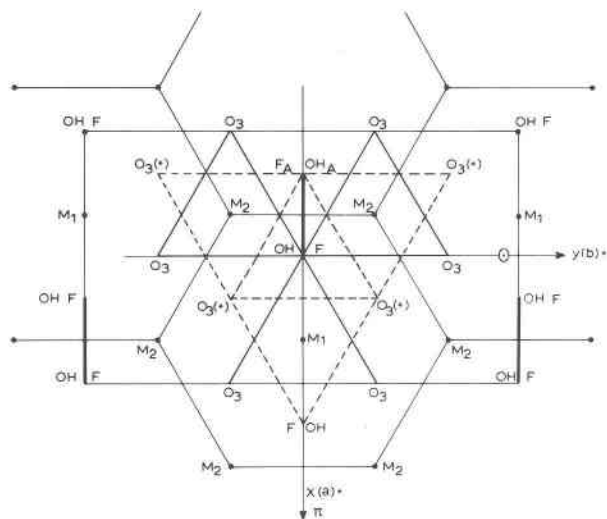

Fig. 1. Projection on the *ab* plane of the octahedral sheet of 1M micas showing the position of OH^-, F^- and *M1* and *M2* sites.

At high frequency, for samples having a high iron and F^- content, weak lines close to the main line can be observed (see Fig. 3); these correspond to OH^- groups which are second neighbors ($r = 4.07A$) to Fe^{2+}. The intensity of these lines is less than that of the first-neighbor lines, although the multiplicity for neighbors is the same. This observation could be explained by a regrouping of certain Fe^{2+} ions, with the result that most of the OH^- groups in these regions will have, in addition to a Fe^{2+} as second neighbor, another Fe^{2+} as first neighbor. This therefore reduces the total contribution of second neighbors to the intensity of their respective side-line. This regrouping of Fe^{2+} ions would also explain why the width of the first-neighbor side-line is larger than that of the main line. By going to lower frequency, this width decreases and approaches that of the main line (see Fig. 3). In the previous analysis of the H^+ side-lines, it was also shown that the substitution of Mg^{2+} by Fe^{2+} is random on the two available sites (this is not in conflict with the above assumed distribution of Fe^{2+} with respect to each other) and that as the iron content increases, the association of OH^- with more Fe^{2+} also increases.

Fluorine signal—a axis

In the F^- spectra obtained at high frequency (56.4 MHz) the side-lines become visible, as in the case for H^+, only when the iron content is above one percent. In this case, however, the side-lines are much closer to the central line (Fig. 4), and their intensity is much less dependent on the Fe^{2+} concentration. At low frequency, the side-lines disappear, being included in

Fig. 3. Example of H^+ NMR signals for sample P-18 showing the principal line and side-lines as function of orientation (*a* axis) and frequency. II corresponds to second-neighbor protons. The upper curves represent the first derivative of the absorption lines.
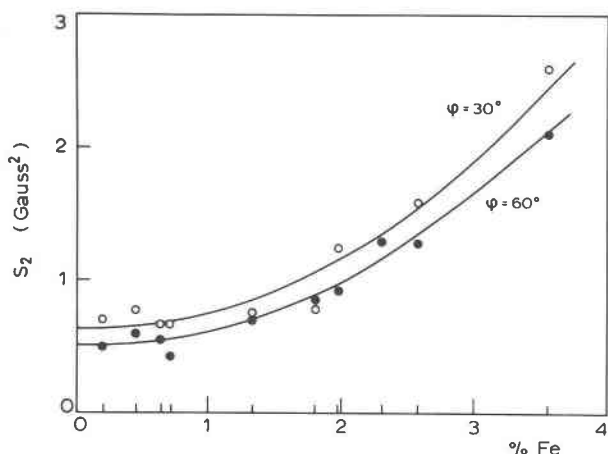

Fig. 2. Experimental second moments of the principal line of H^+ at 60 MHz, as function of the iron content and for two orientations of the C^x axis relative to the applied magnetic field.
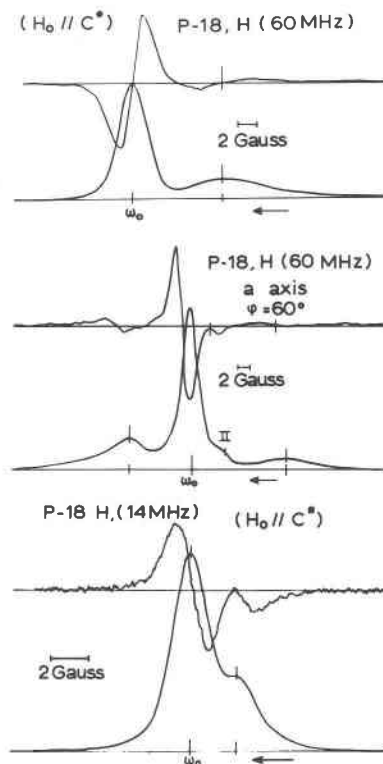
the main central line. Using the same hypothesis as in the previous work (Sanz and Stone, 1977), *i.e.,* a simple time-averaged point dipolar interaction between magnetic moments of iron and nuclei, it is possible to calculate the angular variation of shift that an iron placed either on the *M1* or *M2* site would induce in surrounding F^- nuclei. For this calculation only Fe^{2+} ions are considered, as chemical analysis and Mössbauer spectra (Sanz *et al.,* 1978) have shown that these are the only abundant paramagnetic species present. Moreover, for this analysis the structural model obtained by Joswig (1972) on a phlogopite by neutron diffraction was utilized.

The calculation for the three neighbors (see Fig. 5a) to Fe^{2+} at respectively 2.03, 3.68, and 4.54A has been carried out, and the results for second and third neighbors shown in Figure 5b. Experimentally, in no case have lines corresponding to first-nearest neighbors been seen. The only lines observed at 56.4 MHz are those corresponding to nuclei which are either second or third neighbors to Fe^{2+}. Unfortunately the resolution is not sufficient to be able to distinguish between the two possible sites. These results tend to
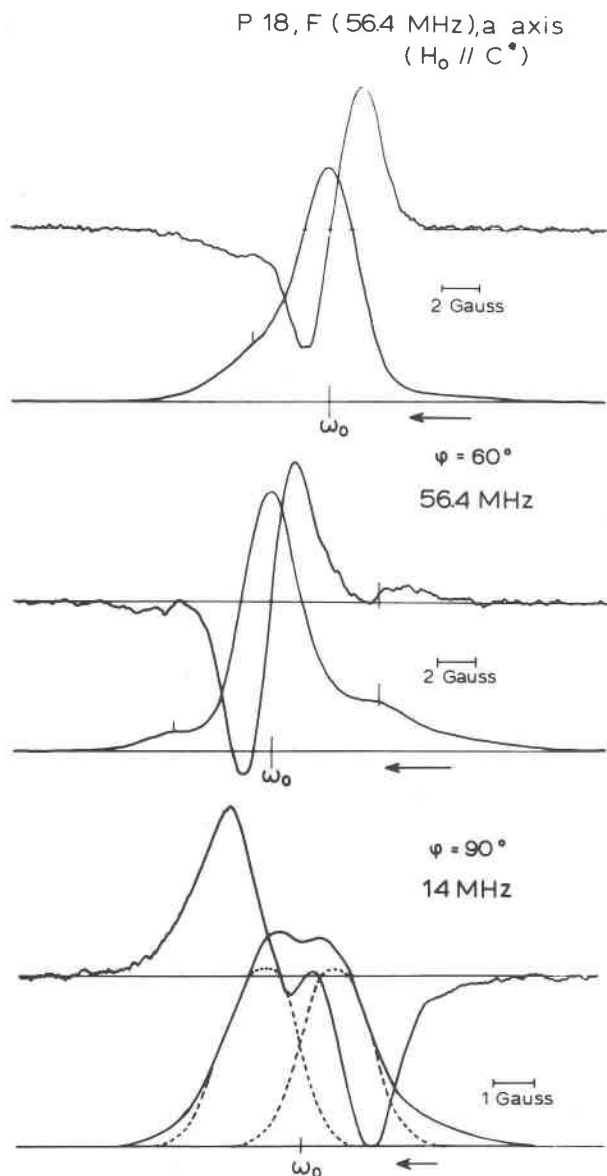
P 18, F (56.4 MHz), a axis
(H_0 // C^*)

Fig. 4. Example of F^- NMR signals for sample P-18 for rotations around the a axis. At high frequency, side-lines are visible. At low frequency, the principal line consists for $\phi = 90°$ of a doublet.

Fig. 5a. Projection in the ab plane showing F^- positions (●) which are at first-neighbor (—), second-neighbor (-----) and third-neighbor (---) distances with respect to $M1$ and $M2$ sites.

the paramagnetic contribution for certain orientations. In samples of high fluorine content (such as P-18), the paramagnetic contribution to the line is less than half as important for the F^- line as it is for the

Fig. 5b. Calculated angular variation of shifts for F^- which are second neighbors to $M1$ (II_1) and $M2$ (II_2) or third neighbors to $M1$ (III_1) and $M2$ (III_2). ●: Experimental points for P-18.

show that unlike OH^-, F^- ions are not directly coordinated to the Fe^{2+} ions.

Moreover, an analysis of the width of the central line shows that the line-width of the F^- line is much more angular-dependent than in the case of H^+. As the paramagnetic contribution is practically rotation-independent, the interaction which is responsible for the width variation must be of another nature, i.e., of diamagnetic origin. This interaction, between nuclear spins only, is observed to be very much larger than
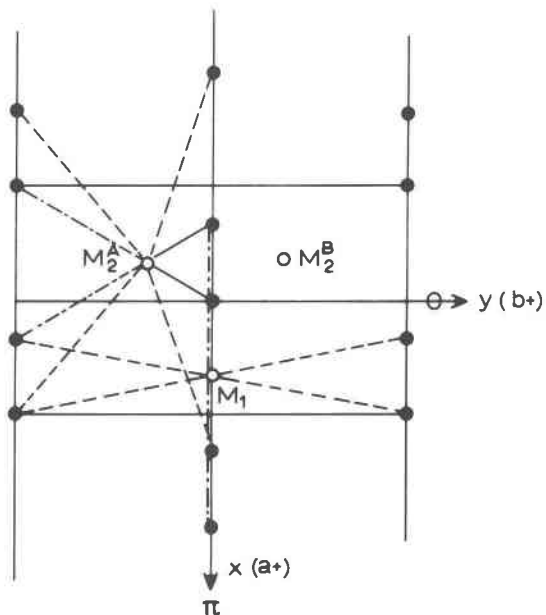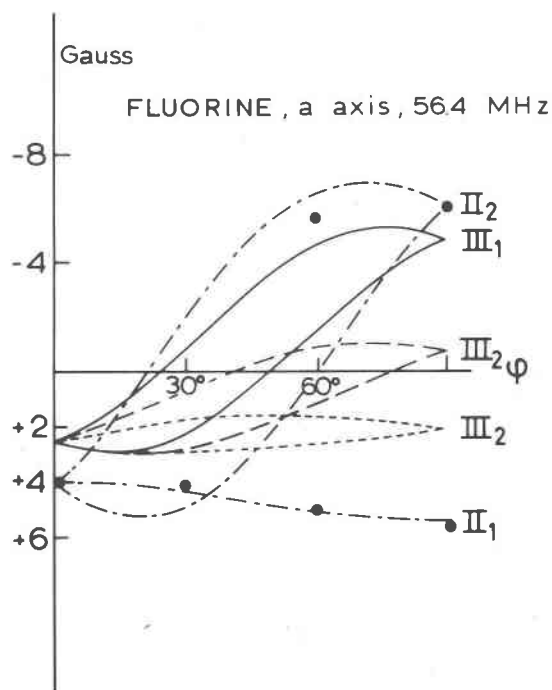
H$^+$ line. This again shows that most of the fluorine ions are more distant from the iron than are the protons.

Finally, when the iron content is sufficiently low, or when the frequency is lowered (Fig. 4), a doublet is observed for certain orientations. A doublet in NMR spectroscopy is the clear indication of a diamagnetic interaction between a pair of spins 1/2, which is the case for H$^+$ and F$^-$. This pair interaction can only be seen if the interaction that each member of the nuclei pair has with its surroundings (*i.e.* electrons or other nuclei such as Al) is less important than the interaction it has with its partner in the pair. The spectra obtained around the *a* axis are poorly resolved, however, and therefore an exact evaluation of the relative importance of the two possible diamagnetic pair interactions, H–F and F–F, as function of the F$^-$ content is difficult. However, this identification will be possible by obtaining spectra while rotating the sample around its *b* axis, as shown in the next section.

In summary, the experiments run around the *a* axis have helped to distinguish between the various interactions involved in the H$^+$ and F$^-$ spectra. They have also shown that, for protons, the paramagnetic contribution is the dominant term at both short (*i.e.* sidelines) and long (central line) distance. For F$^-$ the interactions are on the whole more diamagnetic.

Fluorine signal—b axis

We will discuss here the results obtained at low frequency (14 MHz) for rotations around the *b* axis, which is normal to the π plane containing the F and H atoms. In this case, because of geometrical reasons, the doublet separation associated with these two ions is now larger. This, coupled with the fact that at low frequency the paramagnetic influence on the linewidth is smaller, results in better-resolved spectra. Therefore, it will be much easier to distinguish between the various octahedral associations and also easier to identify the F$^-$ distribution within the octahedral sheet.

The doublet separation, (Pake, 1948), is given by the expression

$$h = \frac{a\mu_1}{r^3}(3\cos^2\theta - 1) \text{ Gauss}$$

where *a* is a constant equal to 3 for two identical spins $I = 1/2$ and equal to 2 for two different spins $I = 1/2$; μ is the magnetic moment of the studied spin; *r* is the internuclear distance; θ the angle between *r* and the applied magnetic field. With the above expression, it is possible to calculate the doublet separation in the case of an interaction between two ions located
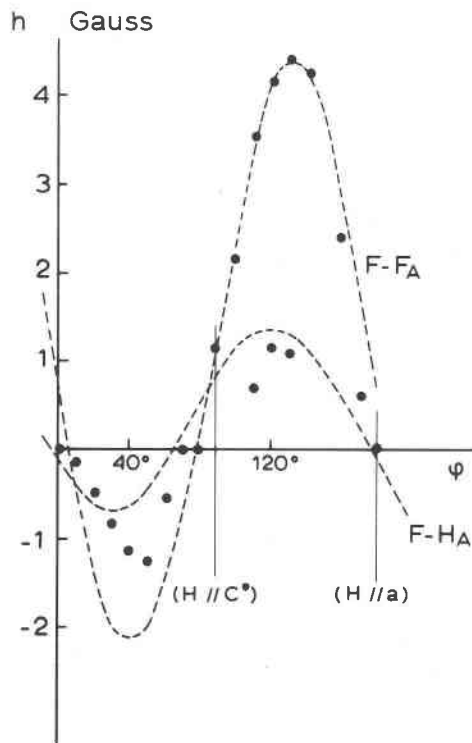

Fig. 6. Calculated angular variation of the F$^-$ doublet separation for F–F$_A$ and F–H$_A$ (rotations around the *b* axis). ●: Experimental points for P-18 with two clearly distinguishable doublet separations from 90° to 180°.

within the same octahedron, F–F$_A$ and F–H$_A$ (Fig. 1); this corresponds to the smallest value for *r*, *i.e.*, 2.64 and 3.45A respectively. The geometrical factors are taken from the structures proposed by Joswig (1972) for phlogopites and McCauley *et al.* (1973) for a fluor-phlogopite.

The results of the calculation are given in Figure 6 by the broken lines for F–F$_A$ and F–H$_A$ respectively. It can be seen that around 130° the two doublet separations are quite different. This orientation is, therefore, very convenient for a quantitative evaluation of the number of associations of both types. Figure 6 also shows the experimental results obtained for sample P-18. For the 90° to 180° region, two doublets can be distinguished clearly with the inner doublet corresponding to F–H$_A$ and the outer doublet to F–F$_A$ (also see Fig. 7); here the agreement is quite good. Because of smaller doublet separation and non-negligible line-widths, from 0° to 90°, the experimental points only reflect an average situation. From the relatively good agreement, it can be concluded that (1) the accuracy with which we could orient our samples is around 5°; (2) the distance
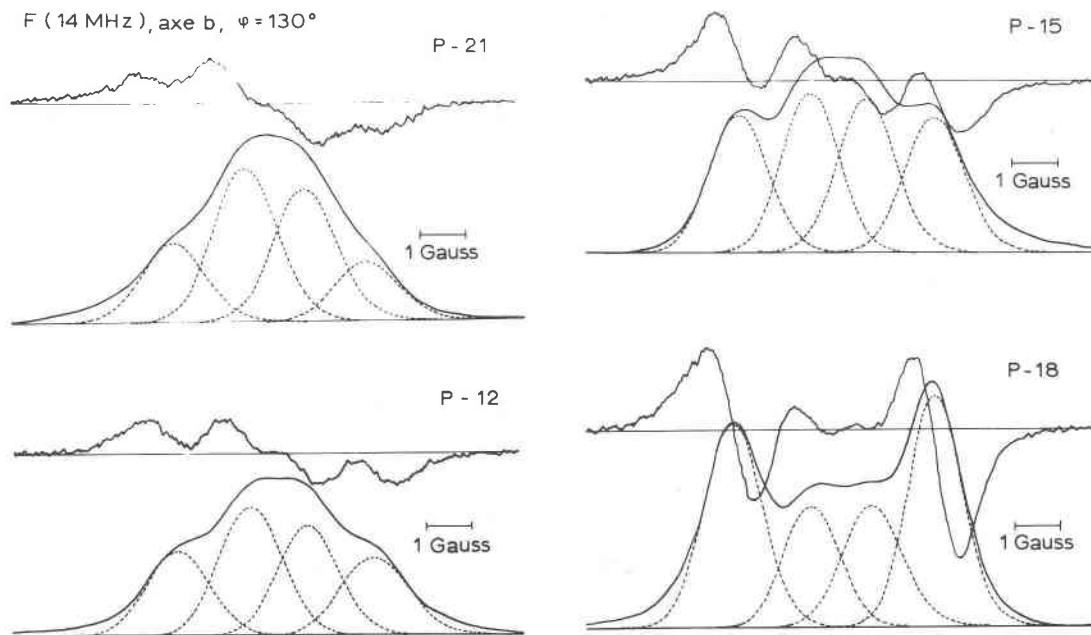
Fig. 7. F⁻ spectra for different phlogopites with increasing content in F⁻: P-21 < P-12 < P-15 < P-18.

2.64A taken for F–F$_A$ from a fluor-phlogopite is quite adequate in our calculation; and (3) complicated polytypism is absent. Concerning this last point, in two cases where frequent stacking faults had been detected by X-ray diffraction, the NMR doublet separation was badly resolved and, because of the various possible orientations for the F–F$_A$ vector, did not follow the expected angular variation; these samples were eliminated from this study.

Eight out of 10 samples were therefore examined around the angle of 130°, in order to study the distribution of F⁻ between the two types of association: F–F$_A$ and F–H$_A$. We observed (Fig. 7) that the intensity

Fig. 8. F–F percentage found for the studied samples (O) as function of the F⁻ content. The broken line curve (---) represents the statistically-calculated values.

of the central doublet (F–H$_A$) decreases relative to the outer doublet (F–F$_A$) as the fluorine content increases. After decomposing our spectra and taking the area under the F–F$_A$ doublet as a measure of the number of F–F pairs, it is possible to compare this figure with the one obtained by taking the mineralogical formula and calculating the probability of finding F–F pairs. This is done in Figure 8, where the experimental and calculated numbers of F–F pairs are given as a function of fluorine content. It can be seen that the number of pairs found experimentally increases much faster at low concentration than is expected from a statistical calculation (40 percent compared to 15 percent for 0.25 F per site). The number of pairs then levels off and finally tends towards the estimated values.
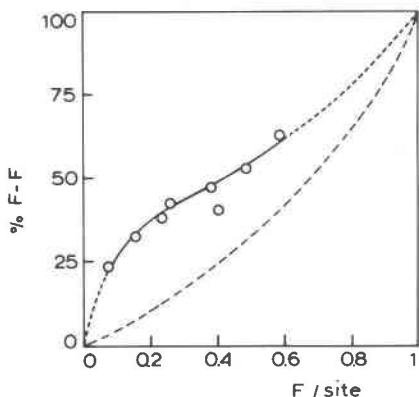
Discussion: octahedral ionic-distribution model

In this work, the identification of the various magnetic interactions responsible for the NMR proton and fluorine spectra has allowed us to differentiate among various octahedral associations. The distribution of elements within these associations was determined by evaluation of the relative importance of each component of the spectral lines. The ability to optimize angular parameters through the use of crystalline samples was important in obtaining this information. Certain important points emerge which will be now discussed.

First, the observation of a rapid increase in the number of fluorine pairs in the domain of very low concentration in F^- can be interpreted as evidence for the existence and prior growth of relatively large fluorine-rich domains. The observation that as the F^- content increases the number of pairs levels off implies that the various domains gradually join together. Since fluorine is only a second- or third-nearest neighbor to Fe^{2+}, these two ions are not directly coordinated to each other, in contrast with the hydroxyl groups, which are found to be located close to the Fe^{2+} ions (nearest neighbor). The fluorine domains, therefore, consist of homogeneous regions containing only Mg^{2+} ions, in which the F–F distance is equal to what is found in a pure fluor-phlogopite. The presence of F^- second-neighbor side-lines of non-negligible intensities, however, suggests that the Fe^{2+} ions are located on the fringe of the F^- domains. The importance of the latter could in principle be estimated by the relative area of the F–OH doublet to the F–F doublet, provided of course the geometry of the domains were known.

The distortion of the octahedral site and the nature and relative distance of surrounding ligands are factors which influence the stabilization energy of a Fe^{2+} ion on its site. In connection with our work, it is perhaps relevant to note that, on the basis of the spectrochemical series (Burns, 1970) and for a given metal and stereochemistry, the ligand field increases when going from F^- to OH^-. This means that OH^- groups form stronger covalent bonds with Fe^{2+}, and consequently that the crystal field energy is higher than it would be for Fe^{2+} sites surrounded by F^- ions only. Note also that in minerals of the humite series, the number of Fe^{2+}-substituted octahedra decreases as the number of F^- ligands increases (Ribbe and Gibbs, 1971).

Sanz and Stone (1977) showed by NMR that the Fe^{2+} ions are distributed randomly on the two possible sites. However, the way the Fe^{2+} ions are distributed relative to each other is also important. The H^+ spectra of the present study show that when the fluorine content is high (P-18), the Fe^{2+} ions tend to group together. Moreover, when the iron content is high, such as in sample P-21 and particularly in biotites (Sanz and Stone, 1977), side-lines due to OH^- groups having several Fe^{2+} ions as first neighbors are observed. This observation provides an interesting means of investigating the iron distribution and also the influence of the F^- content on this distribution. Work in this field on a larger number of samples with a wider range of iron concentration is being pursued.

It seems interesting to compare our approach with X-ray results. X-ray diffraction has clearly shown (Bailey, 1975) the existence, at the unit-cell scale, of cation ordering in the case of 1M mica-related minerals, in which cations of different sizes are located on octahedral sites of different symmetry. For phlogopites such as those studied here, X-ray diffraction does not show such ordering; a random distribution is therefore expected for samples having an octahedral sheet of variable and heterogeneous composition. NMR, however, shows us that OH^- and F^- ions are highly differentiated with respect to cationic associations and that homogeneous fluorine domains are preferred. The chemical homogeneity of these F^- domains is preserved even when the iron content increases drastically (e.g. in biotites; Sanz, 1976). This is not true for the OH^- groups; their environment varies considerably with the Fe^{2+} content, and associations of one, two, or three Fe^{2+} around the same OH^- can be detected (Sanz and Stone, 1977). This heterogeneity of cationic associations around OH^- is clearly visible by IR (Vedder, 1964; Rousseaux et al., 1972), which also shows the association of OH^- groups with highly charged ions (Al^{3+}, Ti^{4+}, etc.). In the octahedral sheet, this local redistribution of cations around the anions does not necessarily follow a regular periodic pattern and therefore cannot be detected by X-ray methods. An interesting case investigated by X-ray which is analogous to phlogopite is the recent study of zinnwaldite (Guggenheim and Bailey, 1977). They found that on one of the three sites of the unit cell, an ordered distribution of octahedral Al exists. This distribution is somewhat favored by the fact that in this mineral there is a quasi-stoichiometric composition of Al in the octahedra. It would be interesting to see if the tendency for F^- to form homogeneous domains such as that shown here also exists in this case, i.e. around cations other than Mg. Only NMR, which directly detects the fluorine pairing, could provide an unambiguous answer. The two methods would therefore be complementary.

Finally, the mutual exclusion relationship of fluorine and iron is an important parameter in the vermiculitization of micas, as the role played by these two ions is known to be quite different. The degree of order–disorder in the distribution of these two octahedral elements could considerably modify the cohesion between layers, and therefore the opening of the latter during the exchange process. This factor added to others as recently reviewed by Giese (1977), i.e. structural distortions, polytypism, number of

vacant sites, *etc.* shows that the alteration process implies more than a simple point-like electrostatic interaction between K^+ and sheet. For a clear understanding of this process, the octahedral sheet should be considered as a whole.

Acknowledgments

References

Bailey, S. W. (1975) Cation ordering and pseudosymmetry in layer silicates. *Am. Mineral., 60,* 175–187.

Burns, R. G. (1970) *Mineralogical Applications of Crystal Field Theory.* Cambridge University Press, Cambridge, England.

Giese, R. F., Jr. (1977). The influence of hydroxyl orientation, stacking sequence and ionic substitutions on the interlayer bonding of micas. *Clays Clay Minerals, 25,* 102–105.

Guggenheim, S. and S. W. Bailey (1977) The refinement of zinnwaldite-1M in subgroup symmetry. *Am. Mineral., 62,* 1158–1167.

Joswig, W. (1972) Neutronenbeugungsmessungen an einem 1M-Phlogopit. *Neues Jahrb. Mineral. Monatsh.,* 1–11.

McCauley, J. W., R. E. Newnham and G. V. Gibbs (1973) Crystal structure analysis of synthetic fluorophlogopite. *Am. Mineral., 58,* 249–254.

Pake, G. E. (1948) Nuclear resonance absorption in hydrated crystals: fine structure of the proton line. *J. Chem. Phys., 16,* 327–336.

Ribbe, P. H. and G. V. Gibbs (1971) Crystal structures of the humite minerals: III. Mg/Fe ordering in humite and its relation to other ferromagnesian silicates. *Am. Mineral., 56,* 1155–1173.

Rousseaux, J. M., C. Gomez-Laverde, Y. Nathan and P. G. Rouxhet (1972) Correlation between the hydroxyl stretching bands and the chemical composition of trioctahedral micas. *Proceedings of the International Clay Conference,* Madrid, Spain, 89–98.

——, P. G. Rouxhet, L. A. Vielvoye and A. J. Herbillon (1973) The vermiculitization of trioctahedral micas. I. K level and its correlation with chemical composition. *Clay Minerals, 10,* 1–16.

Sanz, J. (1976) *Ordre–désordre dans la couche octaédrique des micas trioctaédriques. Etude par RMN, IR et Mössbauer.* Ph.D. Thesis, Université de Louvain, Louvain-la-Neuve, Belgium.

——, J. Meyers, L. A. Vielvoye and W. E. E. Stone (1978) The location and content of iron in natural biotites and phlogopites. A comparison between several methods. *Clay Minerals, 13,* 45–52.

—— and W. E. E. Stone (1977) NMR study of micas. I. Distribution of Fe^{2+} ions on the octahedral sites. *J. Chem. Phys., 67,* 3739–3745.

Vedder, W. (1964) Correlation between infrared spectrum and chemical composition of mica. *Am. Mineral., 49,* 736–768.